Journal of materials and Environmental Sciences
ISSN : 2028-2508

JMES, 2017 Volume 8, Issue 4, Page 1266-1276

http://www.jmaterenvironsci.com/

Study of mass transfer mechanisms for reverse osmosis and nanofiltration membranes intended for desalination

Y.A. Boussouga*, A. Lhassani

Laboratory of Applied Chemistry, Faculty of Science and Technology of Fez, Sidi Mohamed Ben Abdellah University, P.O.Box 2202 Fez, Morocco.

Received 19 Apr 2016,
Revised 27 Oct 2016,
Accepted 31 Oct 2016

Keywords

- ✓ Desalination,
- ✓ Nanofiltration,
- ✓ Reverse Osmosis,
- ✓ Modeling,
- ✓ Mass transfer.

boussouga.youssef@gmail.com ; Phone: +212 6 71 897 313

Abstract

Membrane technologies are increasingly used in water treatment. Nanofiltration and reverse osmosis processes are the most common techniques for desalination of water contaminated by excess of salts. In this present study, we were interested to mass transfer mechanisms which can be made by diffusion or by convection during a filtration process with commercial membranes of nanofiltration (NF90, NF270) and reverse osmosis (BW30, BW30LE and SW30HR). Transport mechanisms of ions through the pores of a membrane in a solvent-salt system were studied by using the model of Spiegler-Kedem-Katchalsky which is based on thermodynamics of irreversible processes. This approach has allowed us to model the observed retention R_{obs} of different salts (NaCl, Na_2SO_4 and $MgSO_4$) with different concentrations (from 10^{-3}M to 10^{-1}M) and to estimate thereafter, the phenomenological parameters for each system membrane/salt: k the mass transfer coefficient, σ the reflection coefficient and Ps the salt permeability. The results showed competitiveness between nanofiltration and low-pressure reverse osmosis membranes, in terms of a selective separation of ions and an important production flux.

1. Introduction

The shortage of drinking water in the future requires an immediate action. The desalination of sea water and brackish water is an alternative solution to deal with this lack [1-2]. Nanofiltration and reverse osmosis are the most used techniques for the demineralization of water contaminated by excess of salts. Nanofiltration is a baromembrane method which is located between ultrafiltration and reverse osmosis. This positioning causes a complexity in term of mass transfer mechanisms; (i) the convection which is under the action of the pressure gradient ΔP and (ii) the diffusion that is realized with the concentration gradient [3].

The experiments of retention were performed on monovalent and divalent salts (NaCl, Na_2SO_4 and $MgSO_4$) at different concentrations and as a function of the transmembrane pressure. Two types of membranes have been studied; nanofiltration membranes (NF270 and NF90) and reverse osmosis membranes which two of them are destined for brackish water (BW30LE and BW30) and one for desalination of sea water (SW30HR). The results were exploited initially by Spiegler–Kedem-Katchalsky model which is a model of irreversible thermodynamics; this modeling aims to determine the phenomenological parameters of mass transfer for each system membrane/salt; the coefficient of reflection σ, salt permeability Ps and the coefficient of mass transfer k [4]. The ions transfer mechanisms were also investigated in a second time with a hydrodynamic model of mass transfer [5]. This approach allowed us to quantify the parts of transfer flow (convection and diffusion) which are characterized by the parameters of mass transfer C_{conv} (the concentration of ions transmitted by convection) and J_{diff} (diffusive flux). A hydraulic characterization of membranes was accomplished by the determination of hydraulic permeability with pure water and saline water. The influence of the concentration on the salts retention has been studied in order to understand the behavior of the membrane during a filtration.

2. Theory

2.1. *Spiegler-Kedem-Katchalsky model*

The Spiegler-Kedem-Katchalsky model is based on the thermodynamics of irreversible process which describes the ion transport mechanism through the pores of a membrane in a solvent-salt system [6]. The equations describe the relation between the solvent flux and the solute flux crossing through nanofiltration or reverse osmosis:

$$J_v = L_p(\Delta P - \sigma\Delta\pi) \quad (1)$$

$$J_s = P_s(C_m - C_p) + (1-\sigma)\,J_v\,C_m \quad (2)$$

With J_v and J_s are respectively the solvent flux and the solute flux. The terms ΔP and $\Delta\pi$ define respectively the transmembrane pressure and osmotic pressure, this last generally depends on the salinity. L_p is the hydraulic permeability with pure water, σ is the coefficient of reflection and P_s represents the salt permeability. The concentrations C_m and C_p are respectively the salt concentration at the surface of the membrane and the salt concentration in permeate. The term $\sigma\Delta\pi$ represents the critical pressure which is the minimum pressure required for a permeate flow [7].

The theoretical curve of salt retention is defined by the following equation [8]:

$$R = \frac{\sigma(1-F)}{1-\sigma F} \quad (3)$$

With: $F = \exp^{-\frac{(1-\sigma)}{P_s}J_v}$ (4)

The equation of the boundary layer theory is expressed by the following relation:

$$\frac{C_m - C_p}{C_0 - C_p} = \exp^{\left(\frac{J_v}{k}\right)} \quad (5)$$

With $k = D_m/\delta$ is the coefficient of mass transfer which is defined by the ratio of the diffusion coefficient D_m and the thickness of the diffusion layer δ. The term C_0 represents the salt concentration in feed. By eliminating the terms of concentrations in Equation 5 with the relations, $R=1-(C_p/C_m)$ and $R_{obs}=1-(C_p/C_0)$ we obtain Equation 6 which describes the relation between the theoretical retention R and the observed retention R_{obs} [9]:

$$\frac{1-R_{obs}}{R_{obs}} = \frac{1-R}{R}\exp^{\left(\frac{J_v}{k}\right)} \quad (6)$$

By introducing Equation 3 into Equation 6, we obtain:

$$R_{obs} = \frac{1}{\dfrac{(1-\sigma)\exp^{\left(\frac{J_v}{k}\right)}}{\sigma\left(1-\exp^{-\frac{(1-\sigma)}{P_s}J_v}\right)}+1} \quad (7)$$

The parameters σ, Ps and k can be estimated by a nonlinear estimation method [9-10], in our case we used the least squares method, this estimation allowed us to obtain a better fit of the theoretical curve which connects the retention salts with the solvent flow.

2.2. *Diffusion and convection of salts*

In Equation 2 there are two terms, the first is the diffusive transport and the second convective transport [5-10]. Therefore, the equation can be written in the following way:

$$J_s = J_v.C_p = J_{diff} + J_v.C_{conv} \quad (8)$$

With $J_{diff} = P_s(C_m - C_p)$ and $C_{conv} = (1-\sigma)C_{\text{int}}$, by dividing Equation 8 with J_v we obtain:

$$C_p = J_{diff}\frac{1}{J_v} + C_{conv} \quad (9)$$

The plot of this equation leads to a line whose the slope corresponds to the diffusive flux of salts J_{diff} and the intercept C_{conv} represents the salt concentration in permeate transmitted by convection.

3. **Materials and methods**

3.1. *Membranes and solutions*

3.1.1. *Membranes studied*

In this work, we have used two types of Filmtec membranes; nanofiltration membranes (NF270 and NF90) and reverse osmosis membranes (BW30LE, BW30 and SW30HR). These membranes are asymmetric and composite; the active layer is composed of polyamide, while the microporous structure and the mechanical support are made from polysulfone. The characteristics of these membranes are given by the supplier in Table 1.

Table 1: Characteristics of different membranes given by the supplier:

Membrane	Supplier	Material	T°C Max	Range of pH	ΔP Max (bar)	Salts retention (%)
NF270	Dow/Filmtec	polyamide	45	3-10	41	40 – 60[(a)]
NF90	Dow/Filmtec	polyamide	45	3-10	41	85 – 95[(b)]
BW30LE	Dow/Filmtec	polyamide	45	2-11	41	99[(c)]
BW30	Dow/Filmtec	polyamide	45	2-11	41	99,5[(d)]
SW30HR	Dow/Filmtec	polyamide	45	2-11	41	99,7[(e)]

(a) Retention of $CaCl_2$ at 500 ppm and $MgSO_4$ at 2000 ppm, (ΔP = 4.9 bars), T = 25°C, Y = 15% (b) Retention of NaCl at 2000 mg/L, (ΔP = 4.9 bars), T = 25°C, Y = 15%. (c) Retention of NaCl at 2000 mg/L (ΔP =15.5 bars), T= 25°C, Y =15%. (d) Retention of NaCl at 2000 mg/L, (ΔP =10 bars), T = 25°C, Y =15%.

The membranes were prepared by immersion in pure water (λ=1 $\mu s.cm^{-1}$) for 48h, to remove any preservative agents from membranes.

3.1.2 *Studied electrolytes*

The different synthetic solutions were prepared by mixing the demineralized water ($1\mu s.cm^{-1}$) with each salt; sodium chloride (NaCl), sodium sulfate (Na_2SO_4) and magnesium sulfate ($MgSO_4$) at different concentrations (10^{-3}M, 10^{-2}M and 10^{-1}M).

3.2. *The filtration unit at laboratory scale*

The tests were carried out on a tangential filtration unit at laboratory scale with a closed system. Permeate and concentrate are recycled to the feed, in order to keep the feed at a constant concentration. The pilot of filtration consists of a stainless steel planar cross flow module provided by GE Osmonics which can support flat RO/NF membranes having a surface of 138 cm². The module also has a hydraulic clamping system to work up to 69 bars of pressure. The unit also has a pump HP (Wanner, USA) which features a feeding circulation speed regulator.

A feed tray has a capacity of 5L and a thermostat for setting the desired temperature. A valve for bypassing the flow of feed and another valve installed at the outlet of the concentrate for fixing the transmembrane pressure by two pressure gauges in the input of the feed and in the output of the concentrate. A flow meter installed at the outlet of the concentrate to adjust the conversion rate. A representative schematic of the equipment is shown in Figure 1.

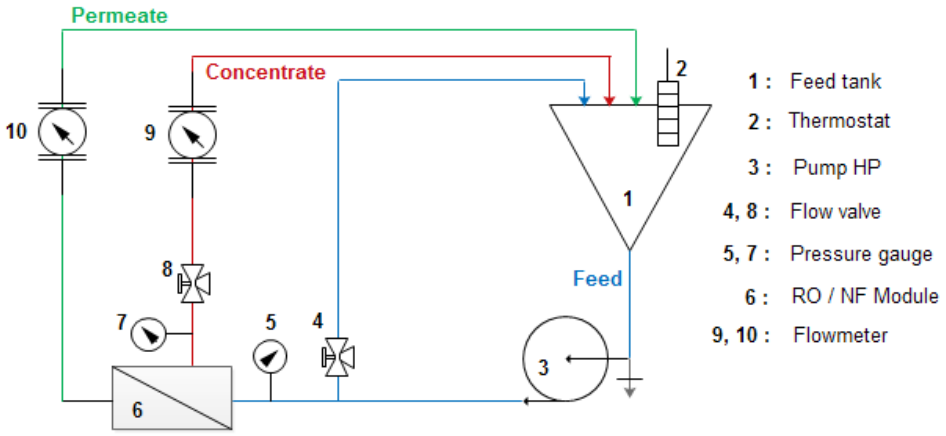

Figure 1: Schematic representation of NF/RO filtration assembly

3.3. *Operational parameters*

The observed rejection rate R_{obs} is a parameter, which allowed evaluating the performance of membrane retention for each salt. It can be written by the following equation:

$$R_{obs} = \left(1 - \frac{C_p}{C_0}\right) \times 100 \quad (10)$$

Changes in concentrations of these salts in the feed C_0, the permeate C_p and the concentrate C_c were followed by conductivity (Conductivimeter Ecoscan) [11].

The conversion rate is calculated by Equation 11 which connects the permeate flux Q_p and the feed flux Q_0:

$$Y(\%) = \left(\frac{Q_p}{Q_0}\right) \times 100 \quad (11)$$

The hydraulic permeability is a parameter which characterizes the productivity of membrane. Being based on Darcy's law, the hydraulic permeability in pure water to a membrane represents the permeate flux as a function of the applied pressure:

$$J_v = L_p \Delta P \quad (12)$$

4. **Results and discussion**

4.1. *Influence of feed concentration on the retention*

The impact of the concentration on the retention of salts has been studied by NaCl and Na_2SO_4 with concentrations between 10^{-3}M and 10^{-1}M. Table 2 below shows the retention of the salts investigated for NF (NF270 and NF90) and for LPRO (BW30LE) with different concentrations at three pressures applied.

In Figure 2, we reveal a clear difference of NaCl retention for the three studied membranes. In nanofiltration, the NF270 gave a retention rate from 18% to 48%, the NF90 from 59% to 69%, while for the low-pressure reverse osmosis membrane BW30LE gave a retention rate between 90% and 82%. The observed deviations between different concentrations may be explained by the phenomenon of concentration polarization [12], which is clearly noticed in the case of the NF270 (Figure 2a) between 10 bars and 15 bars, by against for the case of the BW30LE these deviations are noticed in the low pressure zone (Figure 2c). In the case of Na_2SO_4, Figure 3 shows a slight variation between the results of sulfates retention for different membranes, the variations in retention between the different concentrations are observed in the low pressure area for the three membranes.

In nanofiltration the retention of divalent salts (Na_2SO_4) is higher than monovalent salts (NaCl), this phenomenon can be explained by the hydration energy E_{hyd} which is as function of the ion charge q and the ion radius d [5].

$$E_{hyd} = f\left(\frac{q^2}{d}\right) \quad (13)$$

Table 2: The retention of NaCl and Na_2SO_4 at three pressures, and three different concentrations for NF/LPRO membranes

		R_{obs} (%)								
	Concentration (mol.L^{-1})	0.001			0.01			0.1		
	Pressure (bar)	5	10	15	5	10	15	5	10	15
NaCl	NF270	30	43	48	22	29	33	13	16	18
	NF90	34	55	69	27	49	66	25	47	59
	BW30LE	76	83	90	71	81	87	64	75	82
Na_2SO_4	NF270	91	95	96	90	94	95	88	92	94
	NF90	93	96	98	92	95	97	91	94	95
	BW30LE	94	96	99	93	95	97	91	94	96

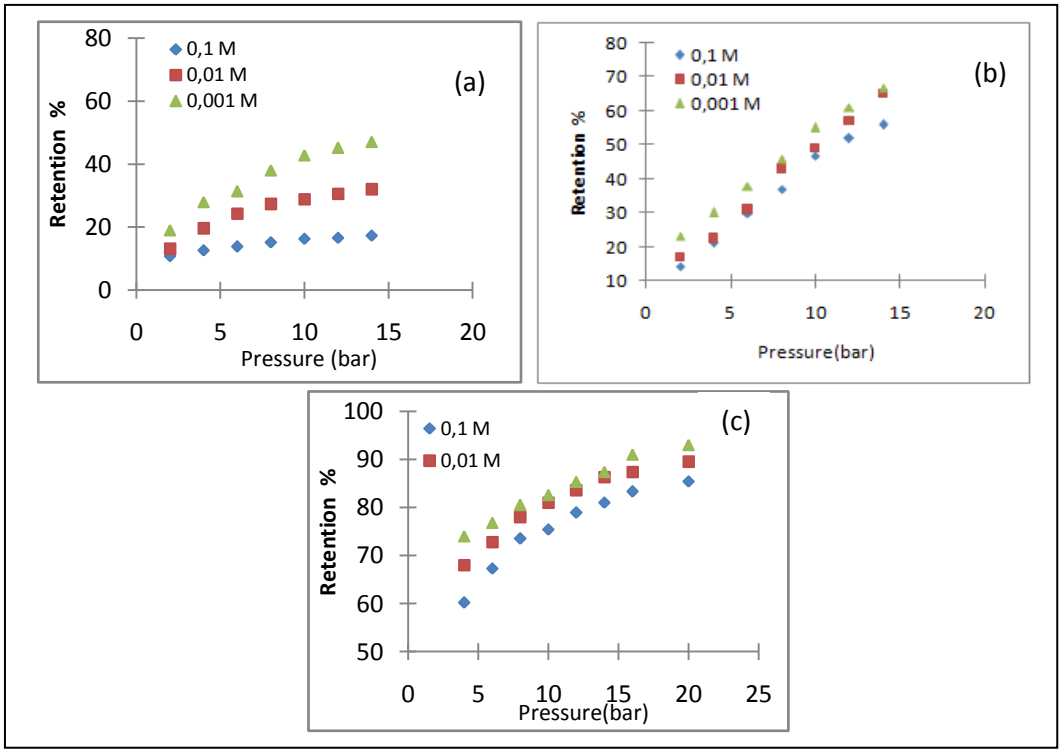

Figure 2: The retention of NaCl as a function of pressure for (a) NF270, (b) NF90) and (c) BW30LE with different concentrations from 10^{-3}M to 10^{-1}M (Y = 5%; T = 24°C)

The hydration energy may also be represented as a function of the molecular weight of the ion M and the ion charge q [5-13]:

$$E_{hyd} = 148 + 556\left(\frac{q^2}{M^{\frac{1}{3}}}\right) + 576\left(\frac{q^2}{M^{\frac{1}{3}}}\right) \quad (14)$$

Whence, we can conclude that the hydration energy is higher for divalent ions, as: $E_{hyd}(SO4^{2-}) > E_{hyd}(Cl^-)$.

4.2. *Modeling of retention for an electrolyte*

The experimental values of the observed retention have been adjusted and analyzed by the mass transport model Spiegler–Kedem-Katchalsky for the different solutions studied [10-14-15-16]. The modeling was based on Equation 7. In Figure 4, we presented the adjustment for NF270 membrane in which the experimental data are marked as full symbols, while the dotted lines represent the SKK model. According to Figure 4, it's clear that there is a very good agreement between the experimental and theoretical results. This method was also used for the other membranes (NF90, BW30LE, BW30 and SW30HR). The estimation of phenomenological parameters k, σ and P_s was achieved through the least squares method. Table 3 represents the estimated values for each membrane with different electrolytes.

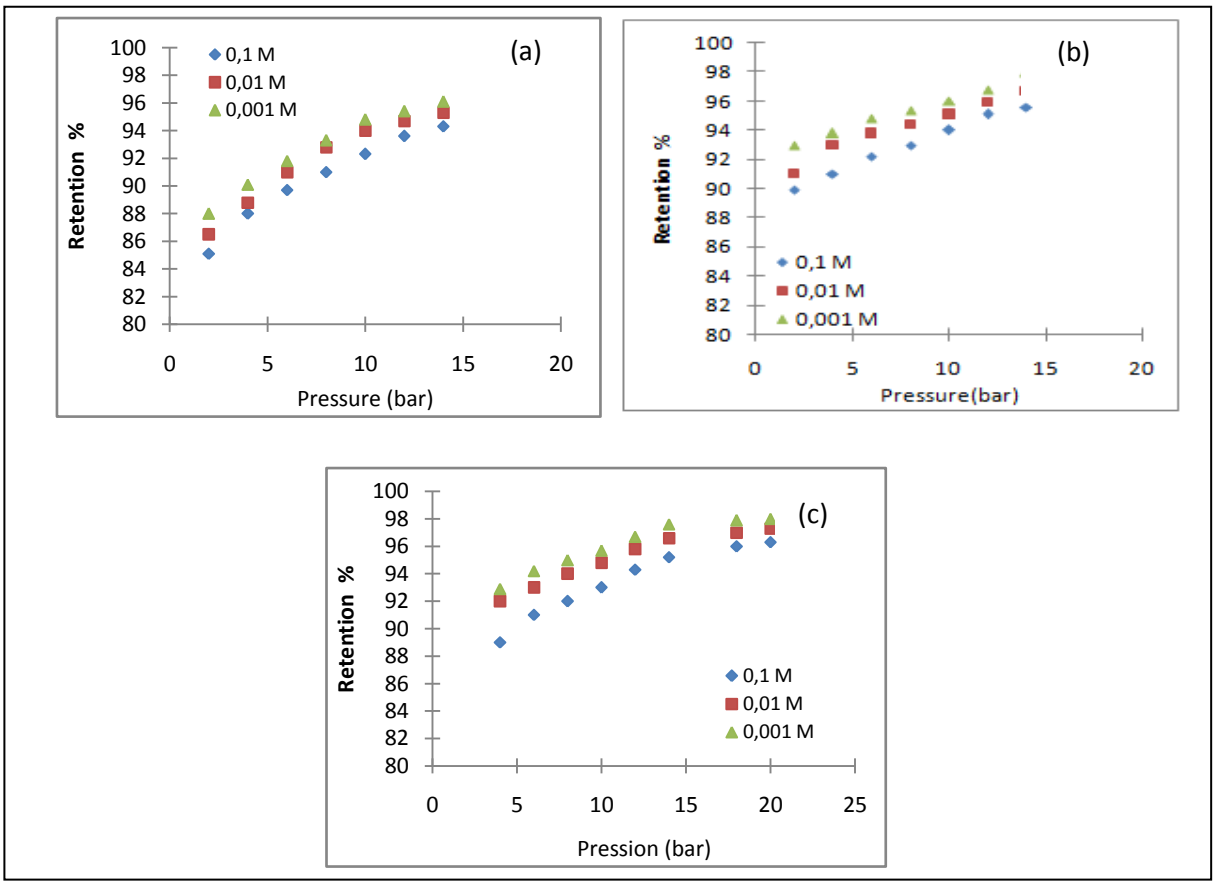

Figure 3: The retention of Na_2SO_4 as a function of pressure for (a) NF270, (b) NF90) and (c) BW30LE with different concentrations from 10^{-3}M to 10^{-1}M (Y = 5%; T = 24°C)

From the results, we see very clearly that the values k, σ and P_s vary for each system membrane/salt and for each given concentration. Knowing that, the reflection coefficient σ takes into consideration the effect of pressure on solute transfer, and it also proportional to the retention. The salt permeability Ps depends on the effective charge of the membrane, the nature of the solute and its concentration. The mass transfer coefficient k depends on physico-chemical properties of the solution and hydrodynamic conditions of the system [3]. We note in Table 3 that the σ values for reverse osmosis membranes are in most cases very close to 1; this means that in this case we reached a perfect retention for all types of salts; we can explain this also that the transfer of ions in this case was performed by diffusion. For the case of nanofiltration membranes, σ is very low in the system NaCl/NF270 which can be explained by the low retention of chloride and their transfer was carried out by convection [10], while the high retention of sulfates led us to a higher reflection coefficient (close to 1) for the systems Na_2SO_4/NF270 and $MgSO_4$/NF270, which one can conclude that the transfer of these ions was done by diffusion. On the other hand, we also noticed that the coefficient σ decreases with the increasing of the concentration.

Table 3: Summary of the phenomenological parameters determined for the various systems membrane/salt

NF/OI	[salt] ($mol.L^{-1}$)	Salt								
		NaCl			Na_2SO_4			$MgSO_4$		
		σ	P_s (10^{-6} m.s^{-1})	k (10^{-4})	σ	P_s (10^{-6} m.s^{-1})	k (10^{-4})	σ	P_s (10^{-6} m.s^{-1})	K (10^{-4})
NF270	10^{-3}	0.53	6.26	11.7	0.96	0.343	26.61	0.96	0.339	35.86
	10^{-2}	0.51	7.77	0.38	0.95	0.418	100.7	0.94	0.263	99.79
	10^{-1}	0.22	3.52	0.41	0.92	0.197	133.4	0.92	0.240	137.02
NF90	10^{-3}	0.97	10	90.51	0.98	0.139	49.74	0.98	0.151	6.39
	10^{-2}	0.97	9.62	25.56	0.97	0.186	142.9	0.95	0.105	192.83
	10^{-1}	0.90	6.13	1.07	0.96	0.198	1050	0.95	0.134	104.47
BW30LE	10^{-3}	0.98	0.525	0.44	0.99	0.111	33.47	0.99	0.142	0.582
	10^{-2}	0.97	1.67	3.11	0.99	0.150	1.08	0.98	0.080	0.19
	10^{-1}	0.96	1.48	1.23	0.97	0.120	0.45	0.97	0.102	0.28
BW30	10^{-3}	0.99	0.267	0.36	0.99	0.106	6.64	0.99	0.054	9.74
	10^{-2}	0.99	1.70	2.64	0.99	0.150	1.08	0.99	0.059	0.22
	10^{-1}	0.98	1.08	0.46	0.98	0.126	6.50	0.98	0.075	0.56
SW30HR	10^{-3}	0.99	0.055	50.56	0.99	0.020	93.31	0.99	0.013	133.1
	10^{-2}	0.99	0.058	17.83	0.99	0.020	1.69	0.99	0.019	1.49
	10^{-1}	0.99	0.051	0.09	0.99	0.015	1.03	0.99	0.015	1.03

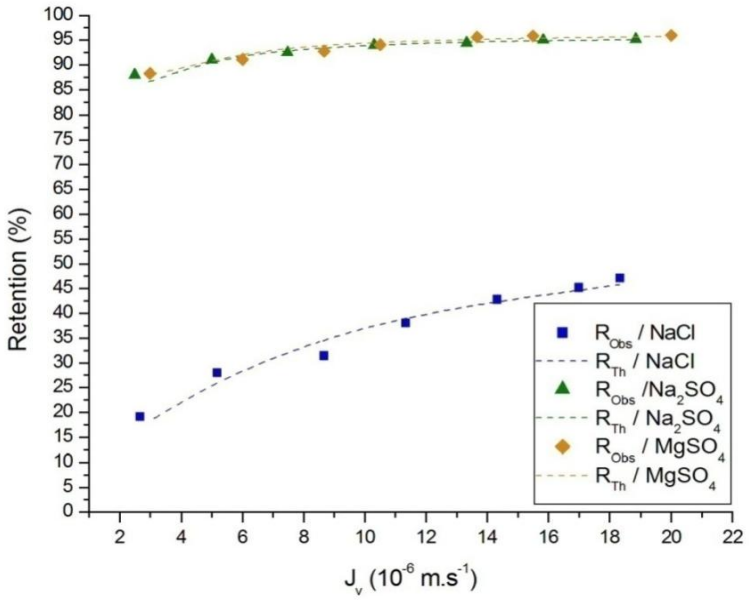

Figure 4: Evolution of retention of NaCl, Na_2SO_4 and $MgSO_4$ as a function of permeate flux for NF270 membrane, the theoretical curve was fitted by the model Spiegler–Kedem-Katchalsky

4.3. *The mass transfer in a system membrane/salt*

The retention of different electrolytes (NaCl, Na_2SO_4 and $MgSO_4$) at different concentrations compared to the studied membranes (NF270, NF90, BW30LE, BW30 and SW30HR) allowed us to quantify experimentally the parameters of mass transfer J_{diff} and C_{conv} which previously mentioned in Equation 9, this method was also treated by different authors [10-13-15-17]. In Figure 5, 6 and 7, the line of the curve shows the evolution of the solute concentration in permeate C_p in function of the inverse of the permeate flux $1/J_v$, the slope of this line represents the part of the transfer flow due to diffusion (J_{diff}), while the y-intercept represents the convective part of global flows (C_{conv}). The values obtained for this study are summarized in Table 4 for the different systems membrane/salt.

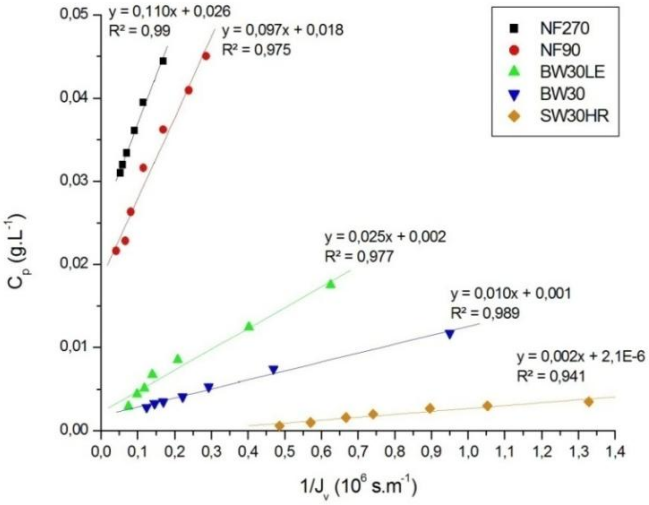

Figure 5: Evolution of C_p as a function of $1/J_v$ for NF and RO membranes (NaCl 10^{-3} M; pH = 6,8; Y = 5%; T = 24°C)

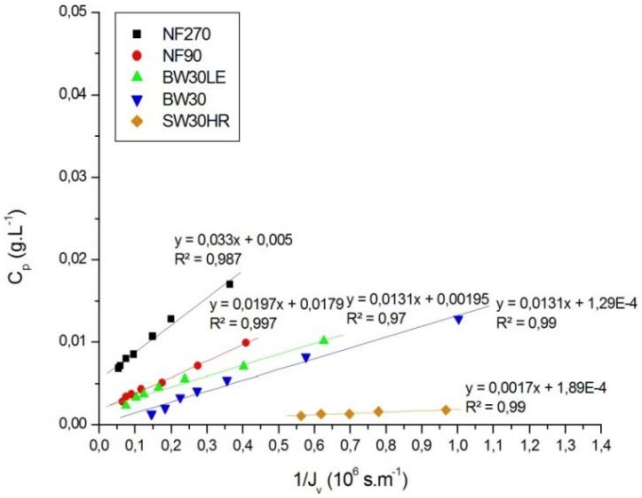

Figure 6: Evolution of C_p as a function of $1/J_v$ for NF and RO membranes (Na_2SO_4 10^{-3} M; pH = 6,8; Y = 5%; T = 24°C)

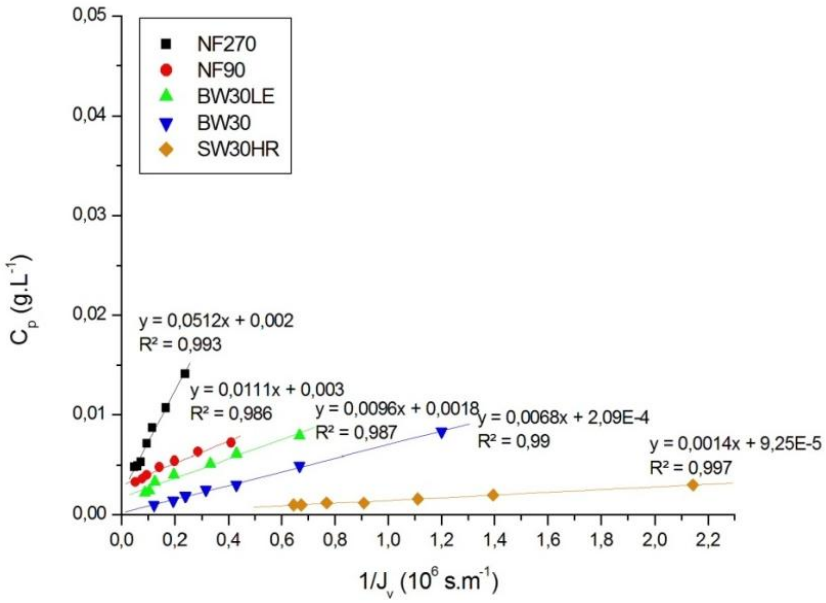

Figure 7: Evolution of C_p as a function of $1/J_v$ for NF and RO membranes ($MgSO_4$ 10^{-3} M; pH = 6,8; Y = 5%; T = 24°C)

Table 4: Values of transfer parameters J_{diff} and C_{conv} for different systems membrane/salt

NF/RO	Salt Concentration ($mol.L^{-1}$)	Salt					
		NaCl		Na_2SO_4		$MgSO_4$	
		C_{conv} ($g.L^{-1}$)	J_{diff} (10^{-6} $m.s^{-1}$)	C_{conv} ($g.L^{-1}$)	J_{diff} (10^{-6} $m.s^{-1}$)	C_{conv} ($g.L^{-1}$)	J_{diff} (10^{-6} $m.s^{-1}$)
NF270	10^{-3}	0.0252	0.1165	0.0054	0.0333	0.0021	0.0511
	10^{-2}	0.3939	0.2894	0.0484	0.4931	0.0589	0.2445
	10^{-1}	4.8735	0.4206	0.8882	1.9549	0.8129	2.0423
NF90	10^{-3}	0.0182	0.0971	0.0018	0.0198	0.0029	0.0111
	10^{-2}	0.2124	0.7946	0.0472	0.1887	0.0443	0.0943
	10^{-1}	2.8714	2.2894	0.5288	1.9820	0.5519	1.1773
BW30LE	10^{-3}	0.0023	0.0250	0.0019	0.0131	0.0017	0.0097
	10^{-2}	0.0341	0.5914	0.0194	0.1693	0.0379	0.0722
	10^{-1}	0.5338	4.2651	0.4811	1.1376	0.5296	0.6619
BW30	10^{-3}	0.0018	0.0107	0.0001	0.0131	0.0002	0.0068
	10^{-2}	0.0253	0.6187	0.0149	0.1636	0.0195	0.0629
	10^{-1}	0.4197	3.5367	0.1700	1.5513	0.1807	0.8014
SW30HR	10^{-3}	2E-06	0.0028	5E-05	0.0019	5E-05	0.0014
	10^{-2}	0.0007	0.0183	0.0008	0.0214	0.0001	0.0156
	10^{-1}	0.0163	0.2665	0.0011	0.1746	0.0725	0.1242

According to the plots obtained for each system membrane/salt at a concentration of 10^{-3} M, we note that the reverse osmosis membranes follow a diffusion transport mode because the values of C_{conv} tend to 0. The diffusive According to the plots obtained for each system membrane/salt at a concentration of 10^{-3} M, we note that the reverse osmosis membranes follow diffusion transport mode because the values of C_{conv} tend to 0. The diffusive mode of transport is more important with high pressure reverse osmosis membrane (SW30HR) compared to other LPRO membranes (BW30 and BW30LE). In nanofiltration membranes, we observed two types of solute transport mode; diffusion and convection. In our case we note that NF270 is more convective than NF90 for different electrolytes studied. Salts transfer was made by diffusion for the case of NF90 in the presence of Na_2SO_4 or $MgSO_4$; by against, it was convective in the presence of NaCl. This is can be explained by the various factors affecting the transport mode of salts through the nanofiltration membranes (ionic strength, type of electrolyte, the transmembrane pressure and the nature of the membrane material) [13-18-19]. It is also noted that we obtained the largest slopes in the case of NaCl as in the case of Na_2SO_4 and $MgSO_4$.

4.4. *Hydraulic permeability in pure water and saline water*

The hydraulic permeability with pure water L_p ($\lambda_{pure\ water}$ =1µs.cm-1) was determined basing on Equation 12. The values of permeate flow J_v obtained from the different studied membranes and their variations in terms of the pressure ΔP which are shown in Figure 8. We have obtained a linear evolution of the flow by varying the transmembrane pressure; it shows that Darcy's law is valid [15].

The hydraulic permeability with saline water was performed for solutions of NaCl and de Na_2SO_4 at a concentration of 10^{-1}M. The evolution of permeate flux as function of the transmembrane pressure is shown in Figures 9 and 10. The linearity of curves confirms the Spiegler-Kedem model. The hydraulic permeability with the electrolyte solution L_p' is obtained from the slope and the x-intercept of the curve represents the critical pressure ($Pc = \sigma\Delta\pi$) which is the minimum pressure required for a permeate flow.

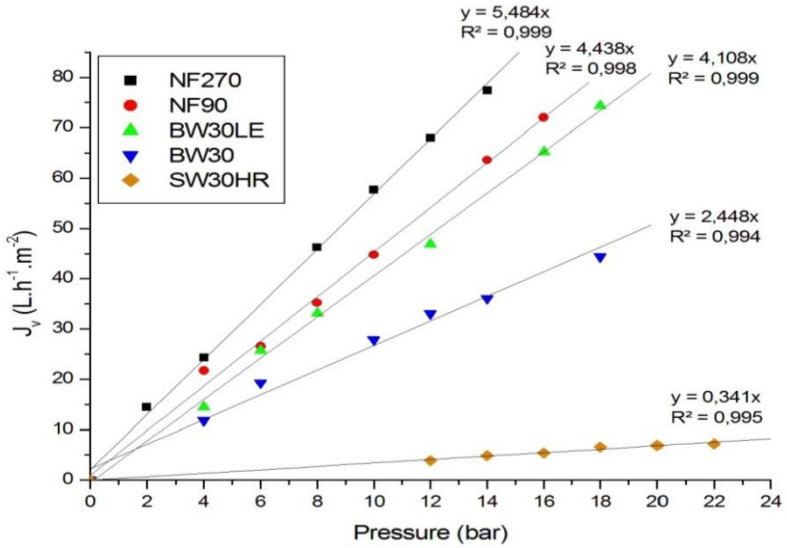

Figure 8: Effect of transmembrane pressure on the permeate flux with pure water for different membranes studied (T=24°, pH=6.5)

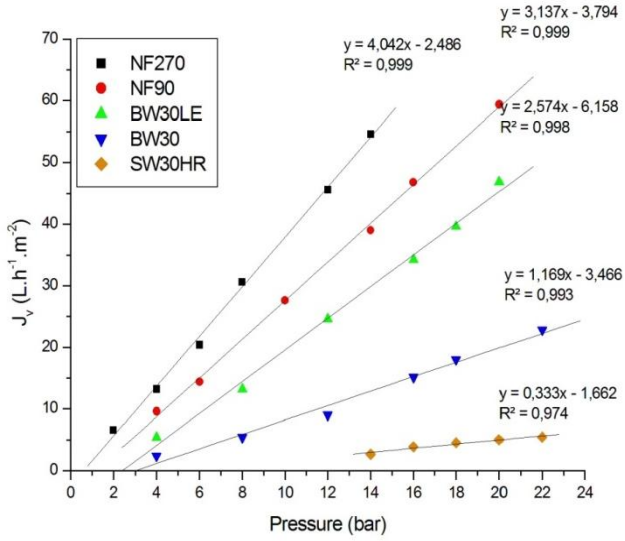

Figure 9: Effect of transmembrane pressure on the permeate flux with NaCl electrolytic solution for different membranes studied ([NaCl] =0.1M, T=24°, pH=6.5)

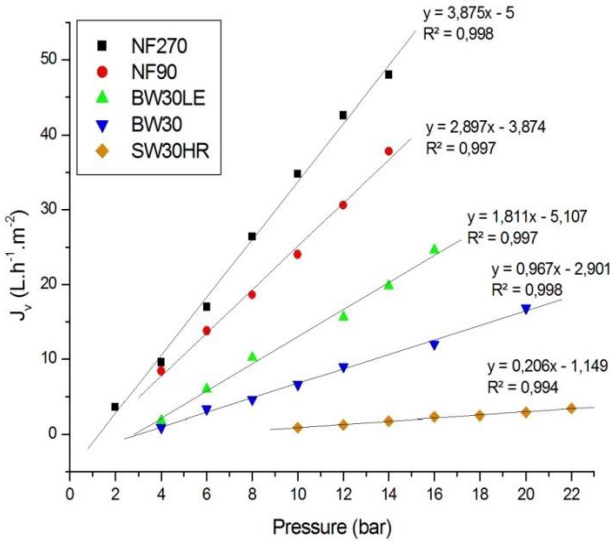

Figure 10: Effect of transmembrane pressure on the permeate flux with Na_2SO_4 electrolytic solution for different membranes studied ([Na_2SO_4] =0.1M, T=24°, pH=6.5)

The results of various cases have shown that the permeate flux for NF membranes is higher compared to RO membranes. In principle, a membrane, which has pores that are more open, will provide more important permeate flux; it's the case of NF270. The parameter values of each membrane, such as, L_p, L_p' and Pc are listed in Table 5.

From the results we can see that the permeability with saline solutions L_p' (NaCl and Na_2SO_4) is less than in the case of pure water L_p, this can be explained by the contraction of the pores in the presence of salts which results the decrease of the permeability [20]. On the other hand, the permeability in the presence of NaCl is higher than that in the presence of Na_2SO_4; this can be explained by the size of the molecule and ion charge (hydration energy).

Table 5: The values of hydraulic permeability with pure water and saline solutions (NaCl and Na_2SO_4) at 0.1M, and critical pressures for NF and RO membranes

Membrane NF/RO	L_p ($L.h^{-1}.m^{-2}.bar^{-1}$)	L_p' ($L.h^{-1}.m^{-2}.bar^{-1}$)		Pc (bar)	
		NaCl	Na_2SO_4	NaCl	Na_2SO_4
NF270	5.48	4.04	3.88	0.62	1.29
NF90	4.44	3.14	2.90	1.21	1.33
BW30LE	4.11	2.57	1.81	2.40	2.82
BW30	2.45	1.17	0.97	2.97	2.99
SW30HR	0.38	0.33	0.21	5.03	5.48

Conclusions

The application of Spiegler-Kedem-Katchalsky model in our study showed that there is good agreement between experimental and theoretical results; the estimated models for nanofiltration membranes and reverse osmosis explain perfectly the phenomenon of salts retention. The retention of sulfates with NF90 (99%) was higher than that using NF270 (96%); this is explained by the fact that the pores sizes of NF90 are lower than those of the NF270. On the other hand, the transfer mode in NF90 is more convective with the presence of chloride, while it is more diffusive with the presence of sulfates. In NF270, the retention of divalent salts (96%) is higher than that of monovalent salts (47%); this is what can be explained by the phenomenon of selectivity. The results also showed competitiveness between NF and RO membranes, given that the NF was effective regarding a selective separation and an important production flux which is represented in our study by the hydraulic permeability.

References

1. Biyoune, M.G., Atbir, A., Bari, H., Mongach, E., Khadir, A., Hassnaoui, L., Boukbir L., El Hadek, M., *J. Mater. Environ. Sci.* 5 (S2) (2014) 2359
2. Goh, P.S., Matsuura, T., Ismail, A.F., Hilal, N., *Desali.* 391 (2016) 43
3. Maurel, A., *Tech. Ing, Génie Proc*. 3J2790 (1993) J2790.1
4. Kedem, O., Katchalsky, A., *Trans. Faraday Soc*. 59 (1963) 1918
5. Lhassani, A., Rumeau, M., Benjelloun, B., *Trib. Eau*. 53 (2000) 100
6. Spiegler, K.S., Kedem, O., *Desali.* 1 (1966) 311
7. Dach, H., *F. S. T. Fès USMBA.* (2008) PhD Thesis
8. Chaudharia L.B., Murthy Z.V.P., *J. Hazar. Mater*. 180 (2010) 309
9. Murthy Z.V.P., Gupta, S.K., *Desali.* 109 (1997) 39
10. Kelewou, H., Lhassani, A., Merzouki, M., Drogui, P., Sellamuthu, B., *Desali.* 277 (2011) 106
11. APHA, Standard Methods for the Examination of Water and Wastewater, 21 (2005) Washington, DC
12. Van Gestel, T., Vandecasteele, C., Buekenhoudt, A., Dotremont, C., Luyten, J., Leysen, R., Van der Bruggen, B., Maes, G., *J. Membr. Sci.*, 209 (2002) 379
13. Diawara, C.K., Lo, S.M., Rumeau, M., Pontie, M., Sarr, O., *J. Membr. Sci.* 219 (2003) 103
14. Jain, S., Gupta, S.K., *J. Membr. Sci.* 232 (2004) 45
15. Pontié, M., Dach, H., Leparc, J., Hafsi, M., Lhassani, A., *Desali.* 221 (2008) 174
16. Wu, F., Feng, L., Zhang, L., *Desali.* 362 (2015) 11
17. Lhassani, A., Rumeau, M., *Trib. Eau.* 52 (1999) 13
18. Szaniawska, D., Spencer, H.G., *Desali*. 101 (1995) 31
19. Lebrun, R.E., Xu, Y., *Sep. Sci. Technol.* 34(8) (1999) 1629
20. Huang, R., Chen, G., Sun, M., Gao, C., *Sep. Purif. Technol.* 58 (2008) 393